

1 **Adaptive evolution of *Moniliophthora* PR-1 proteins towards its**
2 **pathogenicic lifestyle**

3 Adrielle A. Vasconcelos¹; Juliana José¹; Paulo M. Tokimatu Filho¹; Antonio P. Camargo¹;
4 Paulo J. P. L. Teixeira²; Daniela P. T. Thomazella¹; Paula F. V. do Prado¹; Gabriel L. Fiorin¹;
5 Juliana L. Costa³; Antonio Figueira³; Marcelo F. Carazzolle¹; Gonçalo A. G. Pereira^{1*}; Renata
6 M. Baroni¹

7

8 ¹ Departamento de Genética, Evolução, Microbiologia e Imunologia, Instituto de Biologia,
9 Universidade Estadual de Campinas, Campinas, SP, Brazil.

10 ² Departamento de Ciências Biológicas, Escola Superior de Agricultura “Luiz de Queiroz”
11 (ESALQ), Universidade de São Paulo, Piracicaba, SP, Brazil.

12

13 ³ Centro de Energia Nuclear na Agricultura, Universidade de São Paulo, Piracicaba, SP,
14 Brazil

15

16 * Corresponding author: goncalo@unicamp.br

17

18 **Abstract**

19 *Moniliophthora perniciosa* and *Moniliophthora roreri* are hemibiotrophic fungi that harbor a
20 large number of Pathogenesis-Related 1 genes, many of which are induced in the biotrophic
21 interaction with *Theobroma cacao*. Here, we provide evidence that the evolution of PR-1 in
22 *Moniliophthora* was adaptive and potentially related to the emergence of the parasitic lifestyle
23 in this genus. Phylogenetic analysis revealed conserved PR-1 genes, shared by many
24 Agaricales saprotrophic species, that have diversified in new PR-1 genes putatively related to
25 pathogenicity in *Moniliophthora*, as well as in recent specialization cases within both species.
26 PR-1 families in *Moniliophthora* with higher evolutionary rates exhibit induced expression in
27 the biotrophic interaction and positive selection clues, supporting the hypothesis that these
28 proteins accumulated adaptive changes in response to host-pathogen arm race. Furthermore,
29 we show that the highly diversified *MpPR-1* genes are not induced by two phytoalexins,
30 suggesting detoxification might not be their main function as proposed before.

31

32 **Introduction**

33 Pathogenesis Related-1 (PR-1) proteins are part of CAP (cysteine-rich secretory
34 proteins, antigen 5, and pathogenesis-related 1) superfamily, also known as SCP/TAPS

35 proteins (sperm-coating protein/Tpx-1/Ag5/PR-1/Sc7), and are present throughout the
36 eukaryotic kingdom (Cantacessi et al., 2009; Gibbs et al., 2008). In plants, PR-1 proteins are
37 regarded as markers of induced defense responses against pathogens (van Loon et al., 2006).
38 These proteins have also been ascribed roles in different biological processes in mammals,
39 insects, nematodes and fungi, including reproduction, cellular defense, virulence and
40 evasion of the host immune system (Asojo et al., 2005; Chalmers et al., 2008; Ding et al., 2000;
41 Gao et al., 2001; Hawdon et al., 1999; Lozano-Torres et al., 2014; Prados-Rosales et al., 2012;
42 Schneiter & Di Pietro, 2013; Zhan et al., 2003). In *Saccharomyces cerevisiae*, Pry proteins
43 (*Pathogen related in yeast*) bind and export sterols and fatty acids to the extracellular medium,
44 an activity that has also been demonstrated for other proteins of the CAP superfamily through
45 functional complementation assays (Choudhary & Schneiter, 2012; Darwiche, Mène-Saffrané,
46 et al., 2017; Darwiche & Schneiter, 2016; Gamir et al., 2017; Kelleher et al., 2014).

47 The basidiomycete fungi *Moniliophthora perniciosa* and *Moniliophthora roreri* are
48 hemibiotrophic phytopathogens that cause, respectively, the Witches' Broom disease (WBD)
49 and Frosty Pod Rot of cacao (*Theobroma cacao*). Currently, three biotypes are recognized for
50 *M. perniciosa* based on the hosts that each one is able to infect. The C-biotype infects species
51 of *Theobroma* and *Herrania* (Malvaceae); the S-biotype infects plants of the genus *Solanum*
52 (e.g., tomato) and *Capsicum* (pepper); and the L-biotype is associated with species of lianas
53 (Bignoniaceae), without promoting visible disease symptoms (Evans, 1978; Evans, 2007;
54 Purdy & Schmidt, 1996).

55 With the genome and transcriptome sequencing of the C-biotype, 11 *PR-1*-like genes,
56 named *MpPR-1a* to *k*, were identified in *M. perniciosa* (Teixeira et al., 2012). Interestingly,
57 many of these genes are upregulated during the biotrophic interaction of *M. perniciosa* and *T. cacao*,
58 which constitutes a strong indication of the importance of these proteins in the disease
59 process (Teixeira et al., 2012; Teixeira et al., 2014). In this context, efforts have been made to
60 elucidate the role of these molecules during the interaction of *M. perniciosa* with cacao, such
61 as the determination of the tridimensional structure of *MpPR-1i* (Baroni et al., 2017) and the
62 functional complementation of *MpPR-1* genes in yeast *Pry* mutants (Darwiche et al., 2017).
63 These studies revealed that seven *MpPR-1* proteins display sterol or fatty acid binding and
64 export activity, suggesting that they could function as detoxifying agents against plant lipidic
65 toxins (Darwiche et al., 2017).

66 Despite these advances, studies with a deeper evolutionary perspective have not yet
67 been performed for MpPR-1 proteins. Evolutionary analysis can be an important tool for the
68 inference of gene function and the identification of mechanisms of evolution of specific
69 traits, such as pathogenicity. Genes that are evolving under negative selection pressures are
70 likely to play a crucial role in basal metabolism (Oleksyk et al., 2010). On the other hand, genes
71 that are evolving under positive selection may have changed to adjust their function to a
72 relatively new environmental pressure (Manel et al., 2016). Thus, it can be hypothesized that
73 *Moniliophthora* PR-1 might have accumulated adaptive substitutions in response to selective
74 pressures related to a pathogenic lifestyle, and the analysis of these substitutions may reveal
75 protein targets and specific codons that are potentially important for the pathogenicity in
76 *Moniliophthora*.

77 In this study, we performed a two-level evolutionary analysis of *Moniliophthora* PR-1
78 genes: (i) their macroevolution in the order Agaricales, which consists mainly of saprotrophic
79 fungi, being the *Moniliophthora* species one of the few exceptions; (ii) and their
80 microevolution within *M. perniciosa* and its biotypes that differ in host-specificity. By
81 characterizing PR-1 proteins encoded by 22 *Moniliophthora* genomes, reconstructing their
82 phylogenetic history and searching for evidence of positive selection, we identified an
83 increased diversification in these proteins in *Moniliophthora* that is potentially related to its
84 pathogenic lifestyle, as supported by expression data, and also presents cases of species-
85 specific and biotype-specific diversification.

86

87 **Results**

88

89 **Characterization of PR-1 gene families in *Moniliophthora***

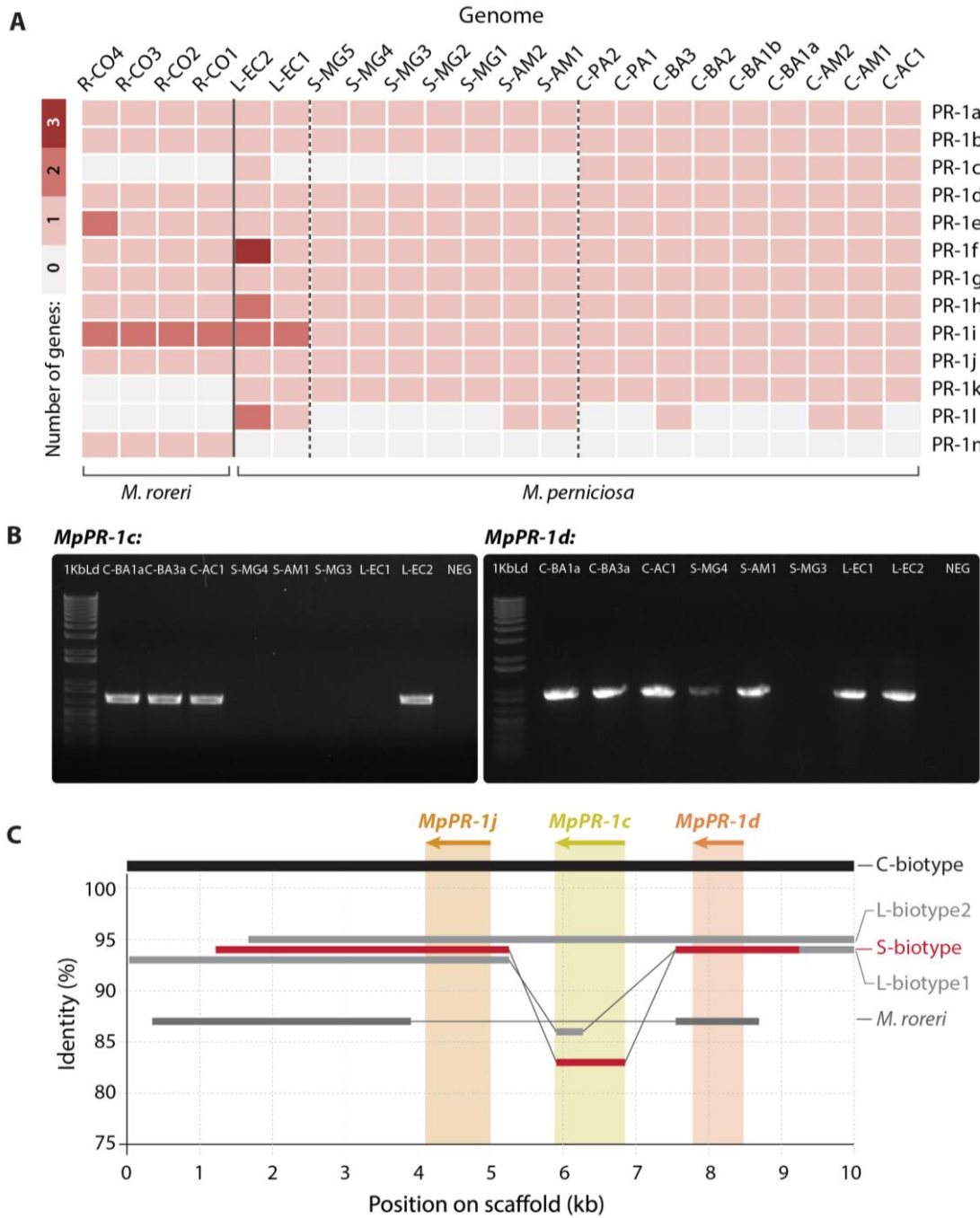
90 Previous work had already reported the identification of 11 PR-1-like genes in the
91 genome of *M. perniciosa* isolate CP02 (C-biotype), which were named *MpPR-1a* to *MpPR-1k*
92 (Teixeira et al., 2012). Likewise, 12 PR-1-like genes were identified in the genome of *M. roreri*
93 (MCA2977) (Meinhardt et al., 2014). With the sequencing and assembly of 18 additional
94 genomes of *M. perniciosa* isolates and other 4 genomes of *M. roreri* isolates, it was possible to
95 characterize the PR-1 gene families in the different biotypes of *M. perniciosa* and in its sister
96 species *M. roreri* in order to look for similarities and differences at the species and biotype
97 levels. Figure 1.A shows the number of genes identified as PR-1 per isolate.

98 The examination of orthogroups containing *PR-1-like* hits revealed that the PR-1i
99 orthogroup has the highest number of duplications with two copies in *M. roreri* and in L-
100 biotype. Moreover, a new PR-1-like orthogroup with seven candidates that are more similar
101 to *MpPR-1i* (67% identity) was found. This newly identified gene was named “*MpPR-1l*” and
102 was not found in *M. roreri*. It has the same number and structure of introns and exons as the
103 *MpPR-1i* gene and they are closely located in the same scaffold, which is evidence of a
104 duplication event within *M. perniciosa*. Interestingly, the sequences corresponding to *MpPR-1l*
105 in the five S-biotype isolates from Minas Gerais were found in another orthogroup, in which
106 *MpPR-1l* was fused to the adjacent gene in the genome (a putative endo-polygalacturonase
107 gene containing the IPR011050 domain: Pectin lyase fold) with no start codon found between
108 the two domains. Furthermore, we found that the *MpPR-1i* gene and, consequently, its
109 predicted protein is truncated in almost all S-biotype isolates from MG (except for S-MG2)
110 (Figure 4).

111 Examining these gene families to look for other putatively species-specific *PR-1* in
112 *Moniliophthora*, we observed that the *MpPR-1k* and *MpPR-1c* genes are not found in the *M.*
113 *roreri* genomes analyzed in this work, while *MrPR-1n* constitutes an exclusive family in this
114 species. The *MrPR-1o* gene previously identified by Meinhardt et al. (2014) was not predicted
115 in any genome as a gene in this work. The protein sequence of *MrPR-1o* has higher identity
116 with *MrPR-1j* (70%), *MpPR-1j* (66%) and *MpPR-1c* (56%), but it is shorter than all 3 protein
117 sequences and does not have a signal peptide like other PR-1 proteins, which suggested that
118 *MrPR-1o* is a pseudogenized paralog of *MrPR-1j*.

119 The absence of *MpPR-1c* in all S-biotype genomes suggested that this gene could be
120 biotype-specific within *M. perniciosa*, however, it was predicted in the L-biotype genome L-
121 EC2. Therefore, we sought to confirm the presence or absence of this gene in different *M.*
122 *perniciosa* by PCR amplification and synteny analysis. The absence of *MpPR-1c* in the S-
123 biotype isolates and in the L-biotype L-EC1 was confirmed, as well as its presence in L-EC2
124 (Figure 1.B). We also amplified the *MpPR-1d* gene, which was predicted in all genomes, in
125 almost all tested isolates, except for S-MG3 because of a mismatch in the annealing regions
126 of both primers. Even though our PCR results indicated that *MpPR-1c* is not present in the S-
127 biotype, synteny analysis of the genome region where *MpPR-1j-c-d* are found in tandem (22)
128 revealed that, in fact, *MpPR-1c* is partially present in these S-biotype genomes (Figure 1.C),

129 suggesting again that the duplication event of PR-1j occurred in the ancestral of *Moniliophthora*
130 but this paralog was also pseudogenized in the evolution of the S-biotype.



131

132 **Figure 1. Characterization of PR-1 gene families in *M. perniciosa* and *M. roreri* genomes. A.**
133 Heatmap of the number of gene copies per family of *PR-1-like* candidates per *Moniliophthora*
134 isolate. Identification of genomes are in columns and PR-1 family names are in rows. **B.**
135 Amplification by PCR of *MpPR-1c* and *MpPR-1d* genes in the genomic DNA of eight *M.*
136 *perniciosa* isolates. 1Kb Ld = 1 Kb Plus DNA Ladder (Invitrogen), Neg = PCR negative control

137 (no DNA). Expected fragment sizes were 687 bp for *MpPR-1c* and 902 bp for *MpPR-1d*. **C.**
138 Synteny analysis of a 10 Kb portion of the genome where the *MpPR-1j*, *c*, *d* genes are found in
139 the three biotypes of *M. perniciosa* and *M. roreri*. The genomes analyzed were C-BA3, S-MG2,
140 R-CO2, L-EC1 and L-EC2. Only identity above 75% to the C-biotype reference is shown.

141

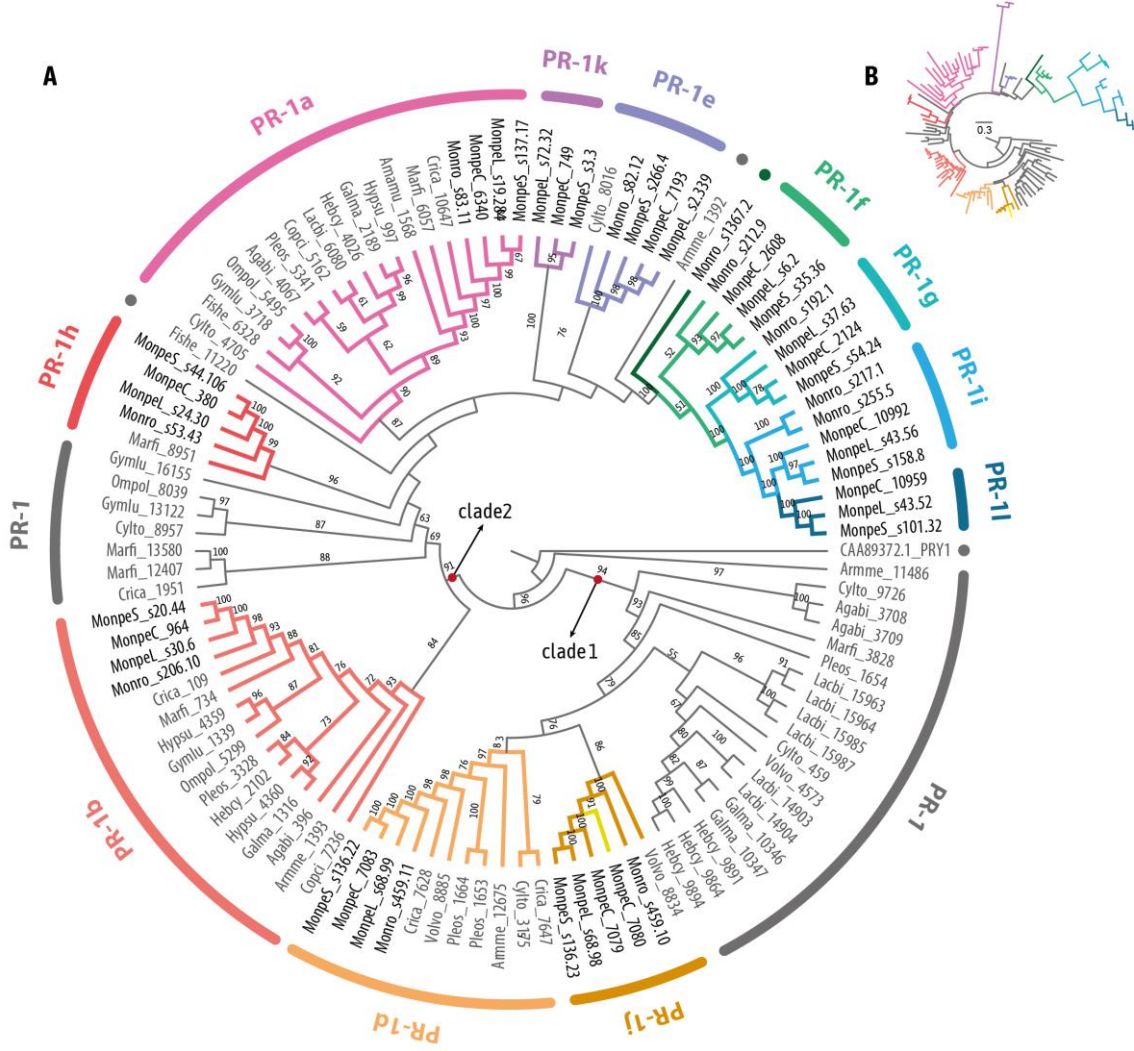
142 **PR-1 genes evolution along the Agaricales order**

143 To study the macroevolution of PR-1 proteins, we identified orthologous sequences of
144 genes encoding PR-1-like proteins in 16 genomes of species from the Agaricales order,
145 including 3 selected *M. perniciosa* genomes (one of each biotype) and 1 *M. roreri* genome for
146 comparisons. The phylogenetic reconstruction of Agaricales PR-1 proteins revealed a basal
147 separation of two major clades, hereafter called clade1 and clade2 (Figure 2.A).

148 The first PR-1 clade includes most Agaricales species outside *Moniliophthora* showing
149 *PR-1* genes that diverged early in the phylogeny, before the appearance of PR-1a-l-n
150 orthologues. From this first clade including the early diverged PR-1 proteins, subsequently
151 diverged PR-1d and PR1-j. The separation between PR-1d and j proposed for *Moniliophthora*
152 only occurs in *Volvariella volvacea*, while for all other species, paralogous of PR-1d diverged
153 early. In *Moniliophthora*, PR-1j and PR-1d have more recent common ancestors, and the only
154 paralogous of these *Moniliophthora* PR-1s originates from a possible duplication of *MpPR-1j*
155 in the C-biotype of *M. perniciosa*, which was previously named *MpPR-1c*, therefore exclusive
156 to this species and biotype.

157 The second clade includes all other PR-1 families and other Agaricales PR-1s that do
158 not have a common ancestor with a single PR-1 from *Moniliophthora*. Clade2 is divided into 2
159 subclasses in its base, one of them composed of the PR-1b clade, which is distributed among
160 14 species. In the second subgroup, PR-1a shows a common ancestor in a total of 16 species,
161 being the most common PR-1 here. The great diversification of a PR-1a-like ancestor in
162 *Moniliophthora* resulted in the formation of at least 4 new and exclusive *PR-1* genes (*k*, *g*, *i*, *l*)
163 with high evolutionary rates reflected on the branch lengths (Figure 2.B). PR-1n showed a
164 putative ortholog in *Armillaria mellea*, the only other plant pathogen in the Agaricales dataset,
165 however, this connection has low branch support.

166



167

168

Figure 2. Phylogenetic cladogram of PR-1 proteins in Agaricales (Basidiomycota). A.

169

170 obtained using 1000 bootstraps. Only branch support values greater than 70 are shown. PR-1c

171

¹⁷² dot and branch. Proteins with ancestral divergences to more than one family were named with

173 the letters of the derived families. Full species names are in SMT. The branch lengths were

174

175

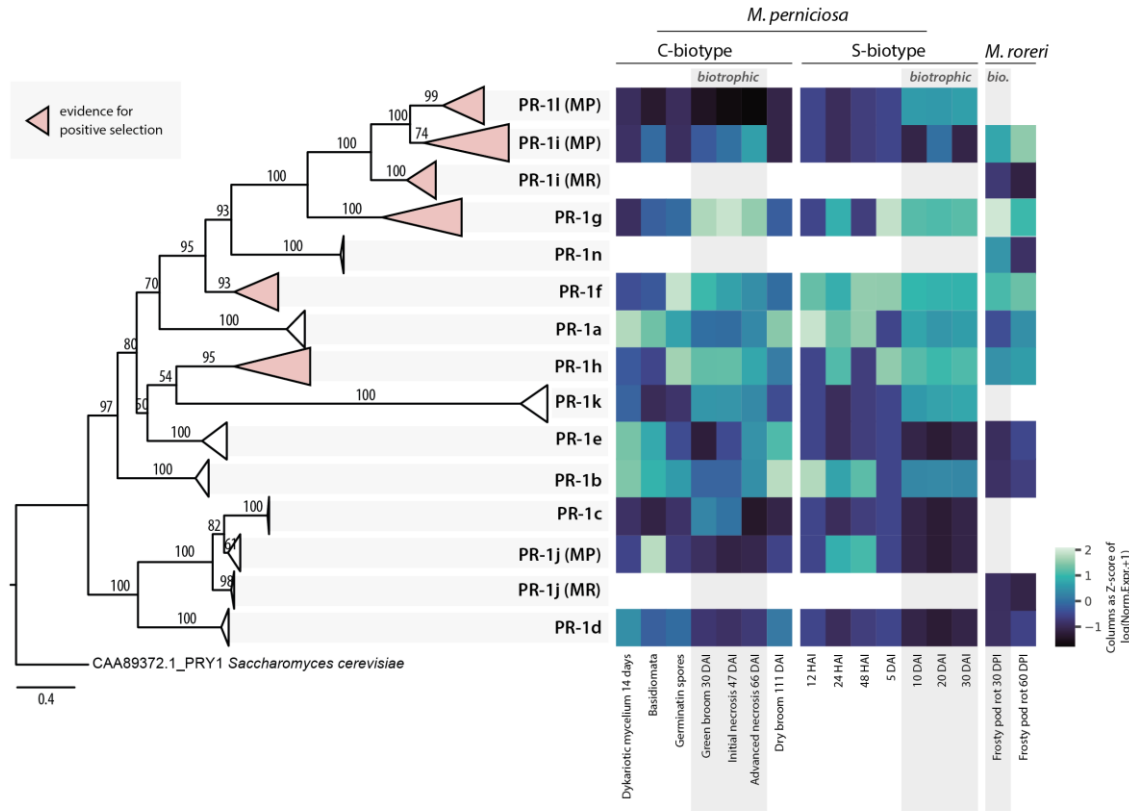
176

177 **Recent diversification of PR-1 genes in *Moniliophthora***

178 Through the investigation of the phylogenetic history of PR-1 proteins within 22
179 *Moniliophthora* isolates (Figure 3), we found that the previous classification of *MpPR-1a* to *k*
180 and *MrPR-1n* represents monophyletic clades in the tree, except for *MpPR-1c* which is a recent
181 paralogous of *MpPR-1j*. The evolution of *Moniliophthora* PR-1 also reflected the basal
182 divergence between two large clades as observed in the Agaricales PR-1 tree (Figure 2). The
183 only incongruence between the two phylogenetic trees is the relative position of PR-1k, which
184 appeared after the divergence of PR-1a in Agaricales and before it in *Moniliophthora*. This
185 incongruence may be due to the extreme differentiation of PR-1k, with longer branch lengths
186 in *Moniliophthora*, being its position on the Agaricales tree more reliable.

187 Among the PR-1 families, the proteins with the greatest number of changes in the tree
188 are PR-1g, i, and k, which are exclusive PR-1s in the genus *Moniliophthora*, as pointed out by
189 the previous phylogenetic analysis. In addition, PR-1h also showed a greater branch length
190 than the others, being a family of PR-1s only shared between *Moniliophthora* and *Marasmium*
191 in the Agaricales PR-1 tree (Figure 2). PR-1c also presented a large number of changes in
192 relation to its ancestor PR-1j. This greater number of changes in these MpPR-1s, and their
193 exclusive presence in comparison to the other Agaricales, indicate a recent potential adaptive
194 process of diversification of these proteins in *Moniliophthora*.

195



196

197 **Figure 3. Phylogenetic reconstruction of PR-1 proteins in *Moniliophthora* and heatmap of**
198 **expression Z-scores of PR-1.** Phylogenetic relationships of PR-1 proteins from 18 *M.*
199 *perniciosa* and 4 *M. roreri* isolates were inferred by maximum likelihood and branch support
200 was obtained using 1000 bootstraps. The PRY1 protein of *Saccharomyces cerevisiae* was used as
201 an outgroup. Clades filled with pink color represent PR-1 families with evidence of positive
202 selection. A version of this tree with non-collapsed branches can be found in Supplementary
203 Figure 1. For each PR-1 family, the Z-score of log transformed expression levels of *MpPR-1*
204 and *MrPR-1* from transcriptomic data was calculated for conditions (columns) and plotted as
205 a heatmap. The heatmap includes *MpPR-1* data from seven conditions of the C-biotype of *M.*
206 *perniciosa* from the Witches' Broom Transcriptomic Atlas, 7 different time points of S-biotype
207 infection in MicroTom tomato plants, and two conditions of *M. roreri* infection in cacao pods
208 (frosty pod rot). Conditions highlighted with a grey background indicate the biotrophic stage
209 of the plant-pathogen interaction.

210

211 **Positive selection shaping PR-1 families in *Moniliophthora***

212 Based on the observations of high diversification of PR-1 families within
213 *Moniliophthora*, we hypothesized that positive selection could be shaping these proteins

214 either in the C-biotype or in the S-biotype. To test this hypothesis, we tested the branch-sites
215 evolutionary model for each PR-1 family. None of these tests brought evidence of positive
216 selection in any PR-1 family for the C-biotype branches. For the S-biotype branches, a signal
217 of positive selection was detected for PR-1g on one site of the protein sequence.

218 Considering that the existence of *M. perniciosa* biotypes are very recent in the
219 evolutionary timescale and that C-biotype itself has almost no genetic variation among its
220 sequences, which makes it very difficult to apply separate dN/dS tests, we tested both C- and
221 S- biotypes together. We tested the hypothesis that there was a single selective pressure
222 shaping PR-1 families throughout the *M. perniciosa* and *M. roreri* evolution regardless of the
223 biotype, using the site model test. In these tests, sites with positive selection signs were
224 detected in five families (PR-1f, g, h, i, l) (Table 2). The PR-1n family was not included in these
225 tests because all sequences were identical.

226

227 **Table 2.** Omega (dN/dS) values and protein sites (amino acid: position) detected with
228 significant probability of positive selection for each PR-1 family in *Moniliophthora*.

Family	Omega	Sites under positive selection (p>0.95)
PR-1a	4.12	None
PR-1b	2.31	None
PR-1c	1	None
PR-1d	2.07	None
PR-1e	1	None
PR-1f	2.74	K: 49, S: 157
PR-1g	7.05	P: 211, P: 234, A: 242, S: 260, S: 271
PR-1h	4.33	S: 78, Y: 107, P: 141, S: 155, E: 187, D: 206, L: 209, M: 224, R: 259, Q: 267
PR-1i	4.38	T: 40, Q: 54, D: 56, R: 118, K: 132, A: 141, L: 150
PR-1l	6.39	Q: 65, Q: 76, -: 164, N: 176, R: 192, K: 193, E: 194, F: 196
PR-1j	2.76	None
PR-1k	2.50	None

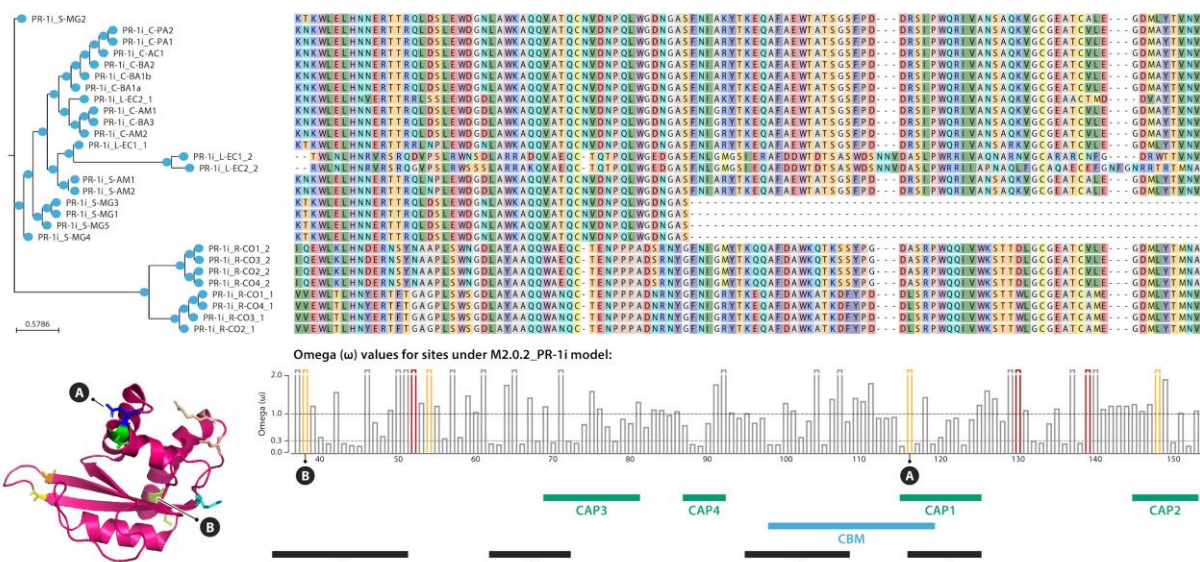
229

230 PR-1g stands out for having the highest omega and for being one of the most expressed
231 genes during the green broom phase (Teixeira et al., 2014). Three of the codons under positive
232 selection are part of the 'keke' domain, which is possibly involved in the interaction with
233 divalent ions or proteins (Teixeira et al., 2012). Among the sites detected under positive
234 selection for PR-1i, one is found in the caveolin binding motif (CBM), an important region for

235 binding to sterols, and another site is in the alpha-helix 1, which together with alpha-helix 4
236 form the cavity for ligation to palmitate (Baroni et al., 2017) (Figure 4).

237 Although the two exclusive PR-1 families of *M. perniciosa*, PR-1c and PR-1k, do not
238 present evidence of positive selection, both revealed processes of diversification in the PR-1
239 phylogenies. It is possible that these families have also undergone selective pressures in their
240 evolution, but the short time of evolution of *M. perniciosa* in relation to the genus has reduced
241 the accuracy of the dN/dS tests in these exclusive families.

242



243

244 **Figure 4. Sequence alignment and phylogeny of PR-1i proteins in *Moniliophthora* isolates.**
245 Only a slice of the middle portion of the alignment is shown to highlight the sites with positive
246 selection signs, indicated by red (p-value ≤ 0.01) or orange (p-value ≤ 0.05) bars in the bar
247 chart of omega values below the alignment. Below the bar chart, annotations indicate the
248 locations along the sequence of the CAP domains, caveolin-binding motif (CBM) and alpha-
249 helices (a). On the 3D crystal structure of MpPR-1i protein (PBD:5V50) and on the bar chart,
250 “A” indicates the site under positive selection detected in the CBM and “B” indicates the site
251 under positive selection in alpha-helix 1.

252

253 Adaptive evolution of PR-1 is reflected on expression data

254 It has already been shown that *MpPR-1* genes of the C-biotype have distinct expression
255 profiles in several different conditions of the WBD Transcriptome Atlas, which were also
256 confirmed by quantitative RT-PCR (Teixeira et al., 2012; Teixeira et al., 2014). *MpPR-1a, b, d,*

257 *e* are ubiquitously expressed during the necrotrophic mycelial stage, while *MpPR-1j* is mainly
258 expressed in primordia and basidiomata. Six *MpPR-1s* are highly and almost exclusively
259 expressed during the biotrophic stage of WBD: *MpPR-1c, f, g, h, i, k* (Teixeira et al., 2012).
260 However, in contrast to *MpPR-1i*, the newly discovered *MpPR-1l* is not expressed in any of the
261 conditions analyzed, suggesting that this gene may not be functional in the C-biotype.

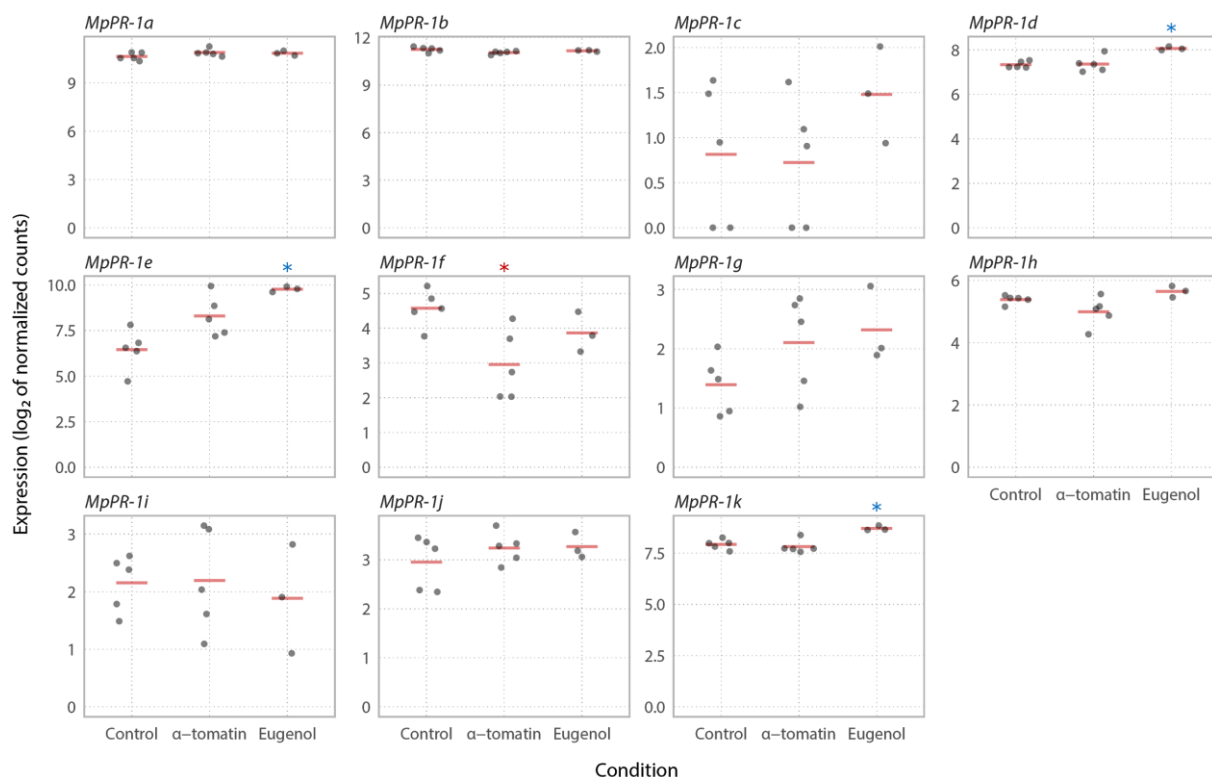
262 Expression data of *MpPR-1* genes from the S-biotype during a time course of the
263 biotrophic interaction with MT tomato revealed that *MpPR-1f, g, h, l*, and *k* are highly
264 expressed during 10-30 days after infection (d.a.i.) (Figure 3). These results are similar to the
265 expression profile verified for the C-biotype during the biotrophic interaction with *T. cacao*,
266 with the exceptions that *MpPR-1c* is absent in the S-biotype and, instead of *MpPR-1i*, *MpPR-1l*
267 is expressed during tomato infection. S-biotype *MpPR-1s* are highly expressed starting at 10
268 d.a.i., which is usually when the first symptoms of stem swelling are visible in MT tomato
269 (Deganello et al., 2014). *MpPR-1a* and *b* appear to have ubiquitous expression profiles since
270 they show similar expression levels in almost all conditions. *MpPR-1j, d, e*, and *i* did not show
271 significant expression in these libraries. Because *MpPR-1i* is truncated in the S-MG1 genome,
272 quantification of expression was also done with S-MG2 as a reference, since it has a complete
273 *MpPR-1i* gene. However, we still obtained the same expression profiles as S-MG1 for all *MpPR-1*.
274 This could suggest that *MpPR-1l* is expressed in S-biotype even with a fusion to the adjacent
275 gene. In the C-biotype, this adjacent gene is only expressed during the biotrophic interaction.

276 In *M. roreri*, it has been previously reported that *MrPR-1n, MrPR-1g* and *MrPR-1i2*
277 were upregulated in samples from the biotrophic phase (30 days post infection of pods),
278 *MrPR-1d* was upregulated in the necrotrophic phase (60 days post infection of pods) and five
279 other *MrPR-1* were constitutively expressed under these conditions (Meinhardt et al., 2014).
280 The heatmap in Figure 3 shows that similar to *M. perniciosa*'s *PR-1* expression profile, *MrPR-1g*
281 is the most expressed *PR-1* gene during the biotrophic stage. Moreover, while *MrPR-1h* and
282 *MrPR-1f* were not differentially expressed when comparing the biotrophic and necrotrophic
283 stages, they also showed higher expression when compared to other *MrPR-1s* that belong to
284 the conserved families.

285

286 **Expression of recently diversified *MpPR-1* was not induced by plant antifungal
287 compounds**

288 It has been previously demonstrated that CAP proteins of *M. perniciosa* bind to a
289 variety of small hydrophobic ligands with different specificities. Thus, it has been suggested
290 that the *MpPR-1* genes induced in the biotrophic interaction could function in the
291 detoxification of hydrophobic molecules produced by the host as a defense strategy
292 (Darwiche et al., 2017). In this context, we investigated if *MpPR-1* genes, especially the ones
293 induced in WBD (*c, f, h, i, k, g*), are differentially expressed by the presence of the plant
294 antifungal compounds eugenol or α -tomatin, which are similar to sterol and fatty acids,
295 respectively. However, when the necrotrophic mycelia of *M. perniciosa* was treated with
296 eugenol, only *MpPR-1e, k, d* were up-regulated, while *MpPR-1f* was down-regulated in α -
297 tomatin-treated samples (Figure 5). In all samples, among all *MpPR-1* genes, *MpPR-1a* and
298 *MpPR-1b* had the highest expression levels, while *MpPR-1c, i, g, j* have the lowest (TPM ≤ 2).
299



301 **Figure 5. Expression profile of *MpPR-1* genes in response to two plant antimicrobial
302 compounds.** The necrotrophic mycelium of *M. perniciosa* C-biotype (C-BA1a) was grown in
303 liquid media in the presence of eugenol, α -tomatin or DMSO (mock condition) for 7 days. The
304 expression values (Log2 transformed) for each *MpPR-1* were obtained by RNA-Seq and

305 subsequent quantification of read counts and between-sample normalization using size
306 factors. Red bars indicate the mean of expression values within a group of replicates.
307 Asterisks indicate that *MpPR-1e, k, d, f* are differentially expressed (s-value<0.005) when
308 compared to the mock condition, with blue asterisk indicating up-regulation and red
309 indicating down-regulation.

310

311 **Discussion**

312 **The evolution of PR-1 and the emergence of pathogenicity among saprotrophs**

313 The plant pathogen *M. perniciosa* has at least 11 genes encoding *PR-1*-like secreted
314 proteins, which were previously identified and characterized in the genome of the C-biotype
315 CP02 isolate (Teixeira et al., 2012). Many of these genes were shown to be highly expressed
316 during the biotrophic interaction of *M. perniciosa* and cacao, suggesting that *MpPR-1* proteins
317 have important roles during this stage of WBD. *M. perniciosa* has two other known biotypes (S
318 and L) that differ in host specificity and virulence, the closest related species *M. roreri* that
319 also is a *T. cacao* pathogen, and other nine *Moniliophthora* species: one described as a non-
320 pathogenic grass endophyte (Aime & Phillips-Mora, 2005), three of biotrophic/parasitic habit
321 (Niveiro et al., 2020), and five species of unascertained lifestyle, found in dead or decaying
322 vegetal substrates (Kerekes et al., 2009; Kropp & Albee-Scott, 2012; Takahashi, 2002). Because
323 the majority of *Moniliophthora* related fungi in the Agaricales order are saprotrophs, the
324 occurrence of parasitic *Moniliophthora* species raises the question about the emergence of
325 biotrophic/parasitic lifestyle in this lineage of Marasmiaceae (Niveiro et al., 2020; Teixeira et
326 al., 2015). The evolutionary scenario of host-pathogen arms race that emerges through the
327 diversification of the *Moniliophthora* genus in the Agaricales order and of host-specific
328 biotypes in *M. perniciosa* isolates, is especially suitable for the study of adaptive evolution in
329 pathogenicity-related genes. Besides, the knowledge on putative adaptations gained through
330 pathogen evolution are also specially interesting for further development of strategies against
331 the pathogen. Based on our findings, Figure 6 presents a model for the adaptive evolution of
332 PR-1 proteins in *Moniliophthora*.

333 Through the characterization of the evolution of PR-1 proteins in Agaricales, we
334 observe that at least one copy of PR-1 is present in all the sampled fungi, with most of the
335 Agaricales species encoding between 1 and 7 PR-1 proteins. This is in contrast with

336 *Moniliophthora* species, which encode among 10-12 proteins. *Moniliophthora* PR-1 proteins
337 are derived independently from both ancient clades in the Agaricales gene tree. The longer
338 branch-lengths in PR-1 families exclusive to *Moniliophthora* along with the evidence of
339 evolution under positive selection identified in independently diverged clades suggest that
340 the diversification of PR-1 in the genus was adaptive and related to its pathogenic lifestyle.
341 The accentuated adaptive evolution of PR-1 in *Moniliophthora* is not only reflected in the
342 genomic evolution of these genes, but also in their expression context. *PR-1c, f, g, h, i, k, l, n*
343 are upregulated during the biotrophic interaction, while *PR-1s* that are also conserved in
344 other Agaricales species are mainly expressed in mycelial stages of *M. perniciosa* (*MpPR-1a,*
345 *b, d, e*). Most Agaricales species are not plant pathogens, which is also an evidence that PR-1
346 in *Moniliophthora* diverged from a few ancestral PR-1s that are related to basal metabolism in
347 fungi and have been evolving under positive selective pressure possibly because of a benefit
348 for the biotrophic/pathogenic lifestyle.

349 The emergence of SCP/TAPs proteins as pathogenicity factors has been reported in
350 other organisms, such as the yeast *Candida albicans* and the filamentous fungus *Fusarium*
351 *oxysporum* (Braun et al., 2000; Prados-Rosales et al., 2012). Even though their specific function
352 and mode of action may be different and remains to be characterized in plant pathogens, the
353 recent evolution of these proteins towards their pathogenic role in the *Moniliophthora* genus
354 could have contributed for the transition from a saprotrophic to parasitic lifestyle.
355 Accelerated adaptive evolution evidenced by positive selection signs has also been observed
356 in other virulence-associated genes of pathogenic fungi, such as the genes *PabaA, fos-1, pes1,*
357 *and pksP* of *Aspergillus fumigatus*, which are involved in nutrient acquisition and oxidative
358 stress response (Fedorova et al., 2008), and several gene families in *C. albicans*, including cell
359 surface protein genes enriched in the most pathogenic *Candida* species (Butler et al., 2009).
360

361 **Adaptive evolution of PR-1 within *Moniliophthora* species and its biotypes**

362 The high diversification of PR-1 families observed within *Moniliophthora* was
363 reinforced by our findings of positive selection in families that have also augmented
364 expressions during infection: PR-1f, g, h, i, l. Among these five families, PR-1g and PR-1i are
365 two of the most diversified families in *Moniliophthora* and have a more recent common
366 ancestor with PR-1f than with the other PR-1s, placing this monophyletic clade of PR-1f, g, i
367 as the key one to diversification and adaptive evolution of these proteins in the genus. Many

368 sites that potentially evolved under selective pressure were also found in PR1-h, indicating
369 that a parallel process of adaptive evolution occurred in this family.

370 Within the diversification of PR-1 in *Moniliophthora*, four cases of putative species-
371 specific evolution of PR-1 families were found: PR-1c, PR-1k and PR-1l in *M. perniciosa* and
372 PR-1n in *M. roreri*. Although vestigial sequences indicate that PR-1c probably emerged as a
373 paralog of PR-1j in the ancestral of both species, it was only kept in the evolution of C-biotype,
374 in which a change in expression profile occurred, thus placing *MpPR-1c* as a case of PR-1
375 diversification within *M. perniciosa* biotypes and a potential candidate for host specificity.
376 Another candidate for biotype-specific diversification is PR-1l, which diverged from a
377 duplication of PR-1i. Even though PR-1l was found in all three *M. perniciosa* biotypes, it was
378 expressed only in the S-biotype during the biotrophic interaction, instead of PR-1i, which is
379 expressed in *M. roreri* and in the C-biotype. This suggests that the divergence of PR-1i can be
380 host-specific, but further experiments are necessary to clarify if they are either a cause or
381 consequence of *M. perniciosa* pathogenicity.

382 Even though almost all PR-1 families are present in the genomes of L-biotype isolates,
383 this biotype has an endophytic lifestyle and does not cause visible disease symptoms in their
384 hosts (H. C. Evans, 1978; Griffith & Hedger, 1994). There is no available expression data for
385 the L-biotype, so it is unknown whether their PR-1 genes could have any role related to their
386 lifestyle or these genes are not pseudogenized yet due to a small evolutionary time. Evans
387 (1978) reported that the L-biotype can induce weak symptoms in seedlings of the Catongo
388 variety of *T. cacao*. Therefore, it could be possible that host susceptibility is an important
389 factor for the manifestation of WBD symptoms.

390

391 **From basal metabolism to key roles in disease: How PR-1 proteins could have 392 functionally adapted for pathogenicity?**

393 It was previously shown that Pry proteins detoxify and protect yeast cells against
394 eugenol (Darwiche, Mène-Saffrané, et al., 2017) and that MpPR-1 proteins can bind to
395 hydrophobic compounds secreted by plants, indicating that they could antagonize the host
396 defense response (Darwiche, El Atab, et al., 2017). When the necrotrophic mycelia of *M.*
397 *perniciosa* was cultivated with eugenol, expression of *MpPR-1d* and *MpPR-1k* was up-
398 regulated, which is in agreement with the ability of these two proteins to bind to plant and
399 fungal sterol compounds (Darwiche, El Atab, et al., 2017). *MpPR-1e* expression was also highly

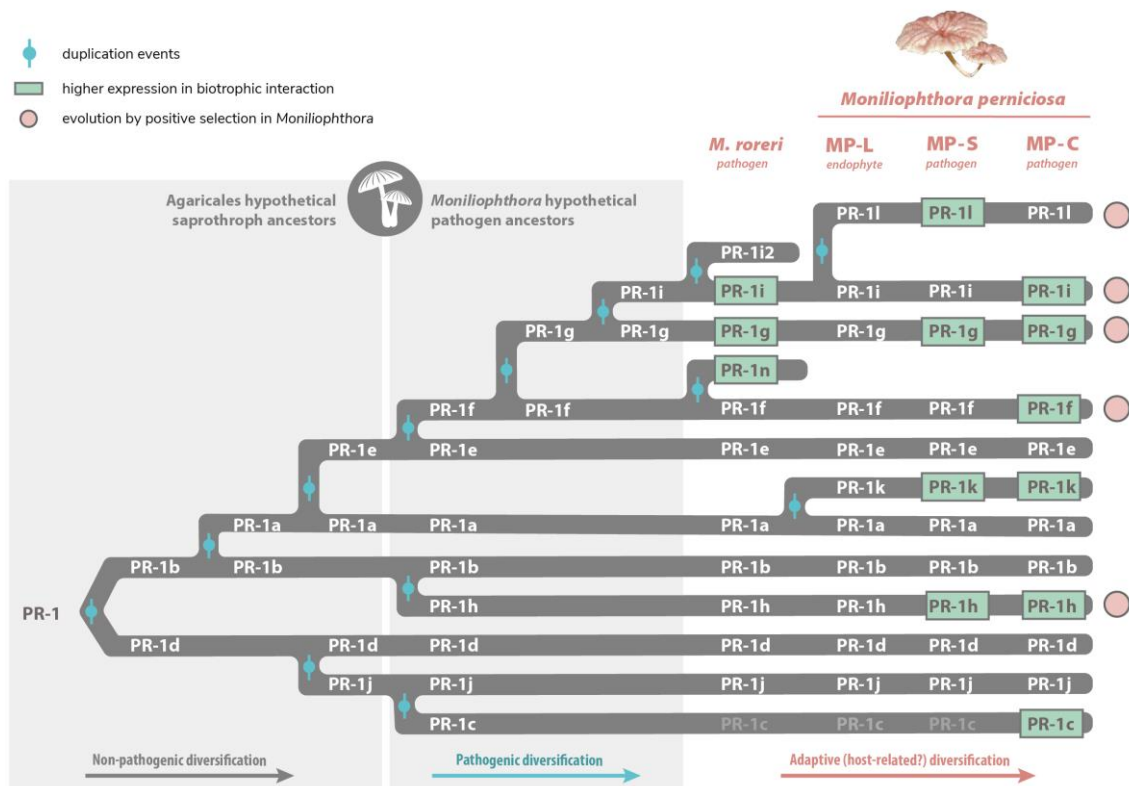
400 induced by eugenol, even though it was previously shown to bind only to fatty acids, but not
401 sterols. Additionally, *MpPR-1f*, which is up-regulated during the biotrophic interaction like
402 *MpPR-1k*, was down-regulated by α -tomatin. Given the above, it appears that *M. perniciosa*
403 does not rely on MpPR-1 for cellular detoxification or this function is not transcriptionally
404 regulated by plant hydrophobic compounds in the necrotrophic mycelia, or even, they could
405 have different roles other than detoxification.

406 Considering that some PR-1 proteins are not associated with infection and are
407 conserved in other saprotrophic fungi, here we hypothesize that the primary function of PR-
408 1 in fungi can be related to the export of sterols from basal metabolism, such as ergosterol,
409 the most abundant sterol in fungal cell membrane (Mohd et al., 2011; Zhao et al., 2005). PRY
410 of *S. cerevisiae* transports acetylated ergosterol to the plasma membrane (Choudhary &
411 Schneiter, 2012) and MpPR-1d, which belongs to a relatively conserved PR-1 family in
412 Agaricales, can also efficiently bind to ergosterol (Darwiche et al., 2017). Furthermore,
413 ergosterol acts as a PAMP molecule (pathogen-associated molecular pattern) in plants
414 (Nürnberg et al., 2004), resulting in the activation of defense-related secondary metabolites
415 and genes, including plant PR-1s (Kasparovsky et al., 2003; Klempner et al., 2014; Lochman
416 & Mikes, 2006; van Loon et al., 2006), which are likely to have a role in sequestering sterols
417 from the membranes of microbes (Gamir et al., 2017) and stress signaling (Chen et al., 2014;
418 Chien et al., 2015). Additionally, PR-1 receptor-like kinases (PR-1-RLK) from *T. cacao* are also
419 upregulated on WBD and could be binding to the same ligand of PR-1 (Teixeira et al., 2013).
420 Given that, it is possible that MpPR-1 could have evolved different adaptive roles through
421 neofunctionalization. Besides export of hydrophobic compounds of basal metabolism, they
422 could be acting in the protection of the cell membrane against the disruption caused by
423 antifungal compounds, in the detoxification of hydrophobic compounds like phytoalexins
424 secreted by the host, or it could even be possible that those *MpPR-1s* expressed during
425 infection are sequestering the membrane sterols of the fungus itself in order to prevent
426 detection by a possible ergosterol recognition complex from the host (Khoza et al., 2019), thus
427 compromising the elicitation of plant immunity in a similar fashion of MpChi, a chitinase-
428 like effector that is highly expressed by *M. perniciosa* during the biotrophic stage of WDB
429 (Fiorin et al., 2018).

430 It has been shown that the ability of MpPR-1 proteins to bind to sterols can be altered
431 by a point mutation in the caveolin binding motif (Darwiche et al., 2017), highlighting the

432 significance of understanding those sites under positive selection that are detected in
433 important regions of the proteins, such as the candidate sites found in the CBM and alpha-
434 helix 1 of PR-1i. These findings are central to learn how changes in the nucleotide or protein
435 sequences could impact binding affinity and function. Even though this is speculative, as the
436 specific role of PR-1 remains unknown, these results can guide further validation
437 experiments and maybe demonstrate another case of adaptive evolution of fungal effectors.
438

438



439

440 **Figure 6. Proposed model for the adaptive evolution of PR-1 proteins in *Moniliophthora***
441 **towards the pathogenic lifestyle.** All *Moniliophthora* PR-1 proteins derived independently
442 from two ancient clades (PR-1b-like and PR-1d-like) within the Agaricales order, as indicated
443 in PR-1 phylogeny. The subsequent diversification of PR-1a and PR-1e from PR-1b, and PR-1j
444 from PR-1d, occurred in putative saprotroph lineages before the divergence of *Moniliophthora*
445 genus, suggesting a diversification not related to pathogenicity. Within *Moniliophthora*
446 hypothetical pathogenic ancestors, five other PR-1 proteins were derived (c from j, h from b,
447 f-g-i from e) and most of these new lineages showed evidence of positive selection in *M.*
448 *perniciosa* samples (indicated by pink circles). New PR-1 copies (n and i2 in *M. roreri*, l and k
449 in *M. perniciosa*) diverged within *M.* species. Recently diversified PR-1 genes in
450 *Moniliophthora*, not only show an elevated rate of evolution and positive selection evidence

451 but are also predominantly expressed during the biotrophic interaction (indicated by green
452 highlights). This supports the hypothesis that these proteins accumulated adaptive changes
453 related to pathogen lifestyle that might also contribute to the host specialization observed in
454 *Moniliophthora* species and biotypes.

455

456 **Conclusions**

457 Based on genomic and transcriptomic data, we presented evidence of adaptive
458 evolution of PR-1 proteins in processes underlying the pathogenic lifestyle in *Moniliophthora*.
459 These results reinforce the power of evolutionary analysis to reveal key proteins in the
460 genomes of pathogenic fungi and contribute to the understanding of the evolution of
461 pathogenesis. Our results indicate a set of PR-1 families that are putatively related to
462 pathogenicity in the genus (PR-1f, g, h, i) and specialization within *M. perniciosa* biotypes (PR-
463 1c, k and l) and *M. roreri* (PR-1n). The positive selection analysis also indicates protein sites
464 that are putatively related to those adaptations. PR-1 genes and sites with evidence of
465 adaptations are strong candidates for further study and should be evaluated in order to
466 understand how changes in these sites can affect structure, binding affinity and function of
467 these proteins.

468

469 **Material and Methods**

470

471 **Identification of PR-1-like gene families**

472 In this study, we used a dataset of families of genes predicted in 22 genomes of
473 *Moniliophthora* (Filho Tokimatu, 2018) and 16 genomes of other fungal species of the order
474 Agaricales, which were obtained from the Joint Genome Institute (JGI) Mycocosm database
475 (Grigoriev et al., 2014). The *Moniliophthora* genomes included are 7 isolates of the S-biotype
476 (collected at the states of Amazonas and Minas Gerais, in Brazil), 9 isolates of the C-biotype
477 (collected at the states of Amazonas, Pará, and Acre, in Brazil), 2 isolates of the L-biotype
478 (from Colombia) and 4 samples of *M. roreri* (from Colombia). Supplementary File 1 contains
479 the list of species and isolates, their genome identification and source (collection location or
480 reference publication).

481 To identify candidate PR-1 gene families, we performed a search for genes encoding
482 the CAP/SCP/PR1-like domain (CDD: cd05381, Pfam PF00188) using the HMMER software

483 (Eddy, 2011). The assignment of protein sequences to families of homologues (orthogroups)
484 was done using Orthofinder (v. 1.1.2) (Emms & Kelly, 2015). In addition, we searched all gene
485 families for families containing *PR-1* candidate genes with Blastp (Camacho et al., 2009) using
486 the known 11 MpPR-1 sequences (Teixeira et al., 2012) as baits, in order to search for possible
487 candidates that were not previously identified and/or that have been wrongly assigned to
488 other orthogroups due to incorrect gene prediction. To verify the presence of the SCP PR1-
489 like/CAP domain (InterPro entry IPR014044) in the sequence, the InterProScan platform
490 (Hunter et al., 2009) was used. All PR-1 candidate sequences identified in this study are
491 deposited in GenBank under accession numbers MW659198 - MW659445.

492

493 **Sequence alignment and phylogenetic reconstruction**

494 For the inference of the phylogenetic history of the gene, the protein sequences of the
495 PR-1 homologue families identified in the 22 *Moniliophthora* isolates were aligned with the
496 PRY1 sequence of *S. cerevisiae* (GenBank ID CAA89372.1), which was used as outgroup.
497 Multiple sequence alignments were performed with Mafft (v. 7.407) (Katoh & Standley, 2013)
498 using the iterative refinement method that incorporates local alignment information in pairs
499 (L-INS-i), with 1000 iterations performed. Then, the alignments were used for phylogenetic
500 reconstruction using the maximum likelihood method with IQ-Tree (v. 1.6.6) (Nguyen et al.,
501 2015), which performs the selection of the best replacement model automatically, with 1000
502 bootstraps for branch support. Bootstraps were recalculated with BOOSTER (v. 0.1.2) for
503 better support of branches in large phylogenies (Lemoine et al., 2018). Likewise, the
504 phylogenetic inference for PR-1 of the Agaricales group of species was performed with the
505 alignment of the homologous proteins identified in the 16 species obtained from Mycocosm,
506 3 isolates of *M. perniciosa* (C-BA3, S-MG3, L-EC1, one representing each biotype), an isolate of
507 *M. roreri* (R-CO1), and PRY1 of *S. cerevisiae* as the outgroup. To improve alignment quality,
508 trimAl package (Capella-Gutiérrez et al., 2009) was used. For dN/dS analysis, considering each
509 gene family independently, the phylogenetic reconstruction was performed using IQ-Tree (v.
510 1.6.6) with the multiple local alignment of the protein sequences obtained with Mafft (v.
511 7.407), and the codon-based alignment of the nucleotide sequences was performed with
512 Macse (v. 2.01) (Ranwez et al., 2018).

513

514 **Detection of positive selection signals**

515 To search for genes and regions that are potentially under positive selection in each
516 of the PR-1 families of the 22 isolates, the CodeML program of the PAML 4.7 package (Yang,
517 2007) was used with the ETEToolkit tool (Huerta-Cepas et al., 2016). CodeML implements a
518 modification of the model proposed by (Goldman & Yang, 1994) to calculate the omega (rate
519 of non-synonymous mutations (dN)/rate of synonymous mutations (dS)) of a coding gene
520 from the multiple alignment sequences and phylogenetic relationships that have been
521 previously inferred.

522 In order to detect positive selection signals in isolates or specific positions in the
523 sequences, we performed tests with the “branch-site” model, which compares a null model
524 (bsA1) in which the branch under consideration is evolving without restrictions (dN/dS = 1)
525 against a model in which the same branch has sites evolving under positive selection (bsA)
526 (dN/dS > 1) (Zhang et al., 2005). In these tests, those branches that were tested for significantly
527 different evolving rates from the others (foreground branches ω_{frg}) are marked in the
528 phylogenetic trees – in this case, the branches corresponding to the isolates of the C-biotype
529 or S-biotype. To detect signs of positive selection at specific sites throughout the sequences,
530 regardless of the isolate, we used the “sites” model (M2 and M1, NSsites 0 1 2) to test all
531 branches of the phylogenetic trees.

532 In both tests, the models are executed several times with different initial omegas (0.2,
533 0.7, 1.2), and the models with the highest probability are selected for the hypothesis test, in
534 which a comparison between the alternative model and the null model is made through a
535 likelihood ratio test. If the alternative model is the most likely one (p-value <0.05), then the
536 possibility of positive selection ($\omega > 1$) can be accepted, and sites with evidence of selection
537 (probability > 0.95) are reported by Bayes Empirical Bayes analysis (BEB) (Zhang et al., 2005).

538

539 **Gene amplification and synteny analysis of PR-1c**

540 In order to confirm the presence or absence of *MpPR-1c* and *MpPR-1d* genes in the
541 genomes of *M. perniciosa* isolates, these genes were amplified by polymerase chain reaction
542 (PCR) from isolates C-AC1, C-BA1a, C-BA3, S-AM1, S-MG3, S-MG4, L-EC1 and L-EC2. The
543 necrotrophic mycelia of these isolates was cultivated in 1.7% MYEA media (15 g L⁻¹ agar; 5 g
544 L⁻¹ yeast extract, 17 g L⁻¹ malt extract) at 28°C for 14 days, then harvested and ground in liquid
545 nitrogen for total DNA isolation with the phenol-chloroform method (Sambrook & Russell,

546 2006). PCRs were performed with primers designed for *MpPR-1c* (F: 5'-
547 GGATCCCGACTTGACAACCTCCATCTCG-3', R: 5'-GAGCTCTCACTCAAACCTCCCCGTCTATAAT-3')
548 and *MpPR-1d* (F: 5'-GGATCCCCCTCGCAATGGGTTTC-3', R: 5'-
549 GTCGACTCAGTCAAGATCAGCCTGGAGA-3') and amplifications cycles consisting of an initial
550 stage of 94°C for 3 min, 35 cycles of 95°C for 30s, 60°C for 50 s and 72°C for 1 min, and final
551 extension at 72°C for 10 min.

552 For synteny analysis, the positions of *PR-1j*, *PR-1c* and *PR-1d* genes were searched in
553 the scaffolds of genomes C-BA3, S-MG2, R-CO2, L-EC1 and L-EC2 by blastn. The scaffolds were
554 then excised 5000bp upstream and 5000bp downstream from the starting position of *PR-1j* in
555 the scaffolds. The resulting 10000 bp excised scaffolds were used for synteny analysis with
556 Mummer (v. 4.0.0beta2) (Kurtz et al., 2004), using the C-BA3 sequence as the reference.

557

558 ***MpPR-1* expression data**

559 *MpPR-1* expression data in RPKM (Reads Per Kilobase per Million mapped reads)
560 values from the C-biotype of *M. perniciosa* in seven biological conditions (dikaryotic mycelium
561 14 days, basidiomata, germinating spores, green broom, initial necrosis, advanced necrosis,
562 dry broom) were downloaded from the Witches' Broom Disease Transcriptome Atlas (v. 1.1)
563 (<http://bioinfo08.ibi.unicamp.br/atlas/>).

564 *MpPR-1* expression data of *M. perniciosa* treated with plant antifungal compounds
565 were obtained from RNA-seq data. The C-BA1a isolate's necrotrophic mycelia was initially
566 inoculated in 100 mL of liquid MYEA media and cultivated for 5 days under agitation of 150
567 rpm at 30°C, then 5 mL of this initial cultivation were transferred to 50 mL of fresh MYEA
568 liquid media containing eugenol (500µM), α-tomatine (80µM) or DMSO (250 µL, solvent
569 control) and cultivated again under agitation of 150 rpm at 30°C for 7 days. The total RNA was
570 extracted using the Rneasy® Plant Mini Kit (Qiagen, USA) and quantified on a fluorimeter
571 (Qubit, Invitrogen). cDNA libraries were prepared in five biological replicates for each
572 treatment, plus biological control. The cDNA libraries were built from 1000 ng of total RNA
573 using Illumina's TruSeq RNA Sample Prep kit, as recommended by the manufacturer. The
574 libraries were prepared according to Illumina's standard procedure and sequenced on
575 Illumina's HiSeq 2500 sequencer. The quality of raw sequences was assessed with FastQC
576 (v.0.11.7). Read quantification was performed by mapping the generated reads against 16084
577 gene models of the C-BA1a genome using Salmon (v.0.14.1) in mapping-based mode (Patro et

578 al., 2017). Read counts were normalized to Transcripts Per Million (TPM) values for plotting.
579 Differential expression analysis was performed with the DESeq2 (v.1.22.2) package using
580 Wald test and Log fold change shrinkage by the *apeglm* method (IfcThreshold=0.1, s-value
581 <0.005) (Love et al., 2014). TPM values and DESeq2 results for *MpPR-1* genes in these
582 experimental conditions are available at Supplementary File 2.

583 *MpPR-1* expression data in TPM for the S-biotype was obtained from RNA-seq libraries
584 of infected MicroTom tomato plants in 7 different time points after inoculation (12h, 24h, 48h,
585 5 days, 10 days, 20 days, 30 days) (Costa et al., under review, Costa, 2017). The quality of raw
586 sequences was assessed with FastQC (v. 0.11.7). Next, Trimmomatic (v.0.36) (Bolger et al.,
587 2014) was used to remove adaptor-containing and low-quality sequences. Quality-filtered
588 reads were then aligned against the S-MG1 or S-MG2 reference genome using HISAT2 (v.2.1.0)
589 with default parameters (Kim et al., 2019). Reads that mapped to coding sequences were
590 counted with featureCounts (v.1.6.3) (Liao et al., 2014). TPM values for *MpPR-1* genes in these
591 experimental conditions are available at Supplementary File 3.

592 *MrPR-1* expression data in TPM was obtained from RNA-Seq reads of *M. roreri* in the
593 biotrophic (30 days after infection) and necrotrophic (60 days after infection) stages of frosty
594 pod rot from (Meinhardt et al., 2014). Reads were mapped and quantified with Salmon
595 (v.0.14.1) (Patro et al., 2017) using 17910 gene models of *M. roreri* MCA 2997 (GCA_000488995)
596 available at Ensembl Fungi.
597

598 **Supplementary Files**

599 **Supplementary File 1. List of fungal genomes and their source (collection site or reference**
600 **publication.** This table contains the species names and biotypes of the fungal genomes used
601 for the identification of *PR-1*-like genes, the identification names we used for the genomes,
602 and their source, which for *M. perniciosa* and *M. roreri* isolates corresponds to their collection
603 site, and for the other Agaricales species corresponds to their reference publication.

604 **Supplementary File 2. *MpPR-1* quantification data and differential expression results of *M.***
605 ***perniciosa* treated with eugenol or alpha-tomatine treatment.** First tab contains a matrix of
606 expression values in Transcripts Per Million (TPM) for *MpPR-1* genes of the necrotrophic
607 mycelia of *M. perniciosa* (C-biotype) treated with eugenol (500 µM), α-tomatine (80 µM) or
608 DMSO (250 µL) (solvent control) for 7 days. Quantification was performed from RNA-Seq

609 reads using the C-BA1a genome as reference. Second tab contains the results table for *MpPR-*
610 1 genes in the differential expression analysis comparing the expression profiles between
611 Eugenol vs Control treatments, while comparison between α -tomatin vs Control treatments is
612 shown in the third tab.

613 **Supplementary File 3. *MpPR-1* expression data in S-biotype infection in tomato.** Matrix of
614 expression values in Transcripts Per Million (TPM) for *MpPR-1* genes of *M. perniciosa* S-
615 biotype infection in MicroTom tomato in various time points of infection (12h, 24h, 48h, 5d,
616 10d, 20d, 30d). Quantification was performed from RNA-Seq reads using the S-MG1 (data in
617 first tab) or S-MG2 genome (data in second tab) as reference.

618 **Supplementary Figure 1. Phylogenetic reconstruction of PR-1 proteins in *Moniliophthora***
619 **isolates (version with non-collapsed branches).** Phylogenetic relationships of PR-1 proteins
620 identified from genomes of 18 *M. perniciosa* and 4 *M. roreri* isolates were inferred by
621 maximum likelihood and branch support was obtained using 1000 bootstraps. The PRY1
622 protein of *Saccharomyces cerevisiae* was used as an outgroup.

623

624 **Funding**

625 This work was supported by the São Paulo Research Foundation (FAPESP) grants to
626 M.F.C (#2013/08293-7), G.A.G.P. and A. F. (#2016/10498-4), and FAPESP fellowships to A.A.V
627 (#2017/13015-7), A.P.C. (#2018/04240-0), P.J.P.L.T. (#2009/51018-1), G.L.F (#2011/23315-1,
628 #2013/09878-9, #2014/06181-0), P.F.V.P. (#2013/05979-5, #2014/00802-2), J.L.C. (#2013/04309-6)
629 and R.M.B (#2017/13319-6).

630

631 **Acknowledgements**

632 We are thankful to Msc. Bárbara A. Pires and Dr. Mario O. Barsottini for helping with
633 the experiments with *M. perniciosa* treated with antifungal compounds and Msc. Leandro C.
634 do Nascimento for performing the assembly of *Moniliophthora* genomes.

635

636 **Competing interests**

637 The authors declare no competing interests.

638

639 **Author contributions**

640 J.J. and R.M.B. conceived and supervised this project. A.A.V. performed identification
641 of PR-1-like candidate genes, evolutionary analysis, and most expression analysis from RNA-
642 seq data, executed PCR experiments and generated figures. P.J.P.L.T. and D.P.T.T. conceived
643 the project of genomics of *Moniliophthora* isolates. P.J.P.L.T., D.P.T.T., P.F.V.P. and G.L.F.
644 executed genomic data acquisition of *Moniliophthora* isolates. J. L.C. executed RNA-seq data
645 acquisition of MT plants infected with S-biotype, and P.J.P.L.T. analyzed this data. P.M.T.F.
646 performed gene prediction, annotation, and assignment of orthogroups from genomes. A. P.
647 C. helped with genomic and RNA-seq analysis. R.M.B. conceived and executed RNA-seq data
648 acquisition of *M. perniciosa* treated with antifungal compounds and A.A.V. analyzed this data.
649 A.A.V. and J.J. wrote the original draft. J.J. and A.P.C. improved the design of figures. J.J.,
650 R.M.B, P.J.P.L.T, D.P.T.T., G.L.F., A.P.C., P.F.V.P. and G.A.G.P. reviewed and edited the draft.
651 M.F.C., A.F. and G.A.G.P. contributed with project supervision and funding acquisition. All
652 authors approved the final manuscript.

653

654 **References**

655 Aime, M. C., & Phillips-Mora, W. (2005). The causal agents of witches' broom and frosty pod
656 rot of cacao (chocolate, *Theobroma cacao*) form a new lineage of Marasmiaceae.
657 *Mycologia*, 97(5), 1012–1022. <https://doi.org/10.3852/mycologia.97.5.1012>

658 Asojo, O. A., Goud, G., Dhar, K., Loukas, A., Zhan, B., Deumic, V., Liu, S., Borgstahl, G. E.
659 O., & Hotez, P. J. (2005). X-ray structure of Na-ASP-2, a pathogenesis-related-1
660 protein from the nematode parasite, *Necator americanus*, and a vaccine antigen for
661 human hookworm infection. *Journal of Molecular Biology*, 346(3), 801–814.
662 <https://doi.org/10.1016/j.jmb.2004.12.023>

663 Baroni, R. M., Luo, Z., Darwiche, R., Hudspeth, E. M., Schneiter, R., Pereira, G. A. G.,
664 Mondego, J. M. C., & Asojo, O. A. (2017). Crystal Structure of MpPR-1i, a SCP/TAPS
665 protein from *Moniliophthora perniciosa*, the fungus that causes Witches' Broom
666 Disease of Cacao. *Scientific Reports*, 7(1), 7818. <https://doi.org/10.1038/s41598-017-07887-1>

668 Bolger, A. M., Lohse, M., & Usadel, B. (2014). Trimmomatic: A flexible trimmer for Illumina
669 sequence data. *Bioinformatics*, 30(15), 2114–2120.
670 <https://doi.org/10.1093/bioinformatics/btu170>

671 Braun, B. R., Head, W. S., Wang, M. X., & Johnson, A. D. (2000). Identification and
672 characterization of TUP1-regulated genes in *Candida albicans*. *Genetics*, 156(1), 31–
673 44.

674 Butler, G., Rasmussen, M. D., Lin, M. F., Santos, M. A. S., Sakthikumar, S., Munro, C. A.,
675 Rheinbay, E., Grabherr, M., Forche, A., Reedy, J. L., Agrafioti, I., Arnaud, M. B.,
676 Bates, S., Brown, A. J. P., Brunke, S., Costanzo, M. C., Fitzpatrick, D. A., de Groot, P.
677 W. J., Harris, D., ... Cuomo, C. A. (2009). Evolution of pathogenicity and sexual
678 reproduction in eight *Candida* genomes. *Nature*, 459(7247), 657–662.
679 <https://doi.org/10.1038/nature08064>

680 Camacho, C., Coulouris, G., Avagyan, V., Ma, N., Papadopoulos, J., Bealer, K., & Madden, T.
681 L. (2009). BLAST+: Architecture and applications. *BMC Bioinformatics*, 10(1), 421.
682 <https://doi.org/10.1186/1471-2105-10-421>

683 Cantacessi, C., Campbell, B. E., Visser, A., Geldhof, P., Nolan, M. J., Nisbet, A. J., Matthews,
684 J. B., Loukas, A., Hofmann, A., Otranto, D., Sternberg, P. W., & Gasser, R. B. (2009).
685 A portrait of the “SCP/TAPS” proteins of eukaryotes—Developing a framework for
686 fundamental research and biotechnological outcomes. *Biotechnology Advances*, 27(4),
687 376–388. <https://doi.org/10.1016/j.biotechadv.2009.02.005>

688 Capella-Gutiérrez, S., Silla-Martínez, J. M., & Gabaldón, T. (2009). trimAl: A tool for
689 automated alignment trimming in large-scale phylogenetic analyses. *Bioinformatics*
690 (Oxford, England), 25(15), 1972–1973. <https://doi.org/10.1093/bioinformatics/btp348>

691 Chalmers, I. W., McArdle, A. J., Coulson, R. M., Wagner, M. A., Schmid, R., Hirai, H., &
692 Hoffmann, K. F. (2008). Developmentally regulated expression, alternative splicing
693 and distinct sub-groupings in members of the *Schistosoma mansoni* venom allergen-
694 like (SmVAL) gene family. *BMC Genomics*, 9(1), 89. <https://doi.org/10.1186/1471-2164-9-89>

695 Chen, Y.-L., Lee, C.-Y., Cheng, K.-T., Chang, W.-H., Huang, R.-N., Nam, H. G., & Chen, Y.-R.
696 (2014). Quantitative Peptidomics Study Reveals That a Wound-Induced Peptide from
697 PR-1 Regulates Immune Signaling in Tomato. *The Plant Cell*, 26(10), 4135–4148.
698 <https://doi.org/10.1105/tpc.114.131185>

699 Chien, P.-S., Nam, H. G., & Chen, Y.-R. (2015). A salt-regulated peptide derived from the CAP
700 superfamily protein negatively regulates salt-stress tolerance in *Arabidopsis*. *Journal*
701 of *Experimental Botany*, 66(17), 5301–5313. <https://doi.org/10.1093/jxb/erv263>

702 Choudhary, V., & Schneiter, R. (2012). Pathogen-Related Yeast (PRY) proteins and members
703 of the CAP superfamily are secreted sterol-binding proteins. *Proceedings of the*
704 *National Academy of Sciences of the United States of America*, 109(42), 16882–16887.
705 <https://doi.org/10.1073/pnas.1209086109>

706 Costa, J. L. (2017). *Patogenicidade e regulação hormonal na interação Moniliophthora perniciosa*
707 x *Solanum lycopersicum* [Tese, Centro de Energia Nuclear na Agricultura,
708 Universidade de São Paulo]. <https://doi.org/10.11606/T.64.2018.tde-04052018-100645>

709 Darwiche, R., El Atab, O., Baroni, R. M., Teixeira, P. J. P. L., Mondego, J. M. C., Pereira, G.
710 A. G., & Schneiter, R. (2017). Plant pathogenesis-related proteins of the cacao fungal
711 pathogen *Moniliophthora perniciosa* differ in their lipid-binding specificities. *The*
712 *Journal of Biological Chemistry*, 292(50), 20558–20569.
713 <https://doi.org/10.1074/jbc.M117.811398>

714 Darwiche, R., Mène-Saffrané, L., Gfeller, D., Asojo, O. A., & Schneiter, R. (2017). The
715 pathogen-related yeast protein Pry1, a member of the CAP protein superfamily, is a
716 fatty acid-binding protein. *The Journal of Biological Chemistry*, 292(20), 8304–8314.
717 <https://doi.org/10.1074/jbc.M117.781880>

718 Darwiche, R., & Schneiter, R. (2016). Cholesterol-Binding by the Yeast CAP Family Member
719 Pry1 Requires the Presence of an Aliphatic Side Chain on Cholesterol. *Journal of*
720 *Steroids & Hormonal Science*, 7(2). <https://doi.org/10.4172/2157-7536.1000172>

721 Deganello, J., Leal, G. A., Rossi, M. L., Peres, L. E. P., & Figueira, A. (2014). Interaction of
722 *Moniliophthora perniciosa* biotypes with Micro-Tom tomato: A model system to
723 investigate the witches’ broom disease of *Theobroma cacao*. *Plant Pathology*, 63(6),
724 1251–1263. <https://doi.org/10.1111/ppa.12206>

725 Ding, X., Shields, J., Allen, R., & Hussey, R. S. (2000). Molecular cloning and
726 characterisation of a venom allergen AG5-like cDNA from *Meloidogyne incognita*.
727 *International Journal for Parasitology*, 30(1), 77–81. [https://doi.org/10.1016/s0020-](https://doi.org/10.1016/s0020-728)

729 7519(99)00165-4
730 Eddy, S. R. (2011). Accelerated Profile HMM Searches. *PLoS Computational Biology*, 7(10),
731 e1002195. <https://doi.org/10.1371/journal.pcbi.1002195>
732 Emms, D. M., & Kelly, S. (2015). OrthoFinder: Solving fundamental biases in whole genome
733 comparisons dramatically improves orthogroup inference accuracy. *Genome Biology*,
734 16(1), 157. <https://doi.org/10.1186/s13059-015-0721-2>
735 Evans, H. C. (1978). Witches' broom disease of cocoa (*Crinipellis perniciosa*) in Ecuador.
736 *Annals of Applied Biology*, 89(2), 185–192. <https://doi.org/10.1111/j.1744-7348.1978.tb07689.x>
737 Evans, Harry C. (2007). Cacao Diseases—The Trilogy Revisited. *Phytopathology*®, 97(12),
738 1640–1643. <https://doi.org/10.1094/PHYTO-97-12-1640>
739 Fedorova, N. D., Khaldi, N., Joardar, V. S., Maiti, R., Amedeo, P., Anderson, M. J., Crabtree,
740 J., Silva, J. C., Badger, J. H., Albarraq, A., Angiuoli, S., Bussey, H., Bowyer, P., Cotty,
741 P. J., Dyer, P. S., Egan, A., Galens, K., Fraser-Liggett, C. M., Haas, B. J., ... Nierman,
742 W. C. (2008). Genomic Islands in the Pathogenic Filamentous Fungus *Aspergillus*
743 *fumigatus*. *PLOS Genetics*, 4(4),
744 e1000046. <https://doi.org/10.1371/journal.pgen.1000046>
745 Filho Tokimatu, P. M. (2018). *Estudo da evolução da fitopatogenicidade em Moniliophthora*
746 *perniciosa através de análises de genômica comparativa de seus biótipos* [Universidade
747 Estadual de Campinas]. <http://repositorio.unicamp.br/jspui/handle/REPOSIP/334998>
748 Fiorin, G. L., Sánchez-Vallet, A., Thomazella, D. P. de T., do Prado, P. F. V., do Nascimento,
749 L. C., Figueira, A. V. de O., Thomma, B. P. H. J., Pereira, G. A. G., & Teixeira, P. J. P.
750 L. (2018). Suppression of Plant Immunity by Fungal Chitinase-like Effectors. *Current*
751 *Biology: CB*, 28(18), 3023-3030.e5. <https://doi.org/10.1016/j.cub.2018.07.055>
752 Gamir, J., Darwiche, R., Van't Hof, P., Choudhary, V., Stumpe, M., Schneiter, R., & Mauch,
753 F. (2017). The sterol-binding activity of PATHOGENESIS-RELATED PROTEIN 1
754 reveals the mode of action of an antimicrobial protein. *The Plant Journal: For Cell and*
755 *Molecular Biology*, 89(3), 502–509. <https://doi.org/10.1111/tpj.13398>
756 Gao, B., Allen, R., Maier, T., Davis, E. L., Baum, T. J., & Hussey, R. S. (2001). Molecular
757 characterisation and expression of two venom allergen-like protein genes in
758 *Heterodera glycines*. *International Journal for Parasitology*, 31(14), 1617–1625.
759 [https://doi.org/10.1016/s0020-7519\(01\)00300-9](https://doi.org/10.1016/s0020-7519(01)00300-9)
760 Gibbs, G. M., Roelants, K., & O'Bryan, M. K. (2008). The CAP superfamily: Cysteine-rich
761 secretory proteins, antigen 5, and pathogenesis-related 1 proteins--roles in
762 reproduction, cancer, and immune defense. *Endocrine Reviews*, 29(7), 865–897.
763 <https://doi.org/10.1210/er.2008-0032>
764 Goldman, N., & Yang, Z. (1994). A codon-based model of nucleotide substitution for protein-
765 coding DNA sequences. *Molecular Biology and Evolution*, 11(5), 725–736.
766 <https://doi.org/10.1093/oxfordjournals.molbev.a040153>
767 Griffith, G. W., & Hedger, J. N. (1994). Spatial distribution of mycelia of the liana (L-) biotype
768 of the agaric *Crinipellis perniciosa* (Stahel) Singer in tropical forest. *New Phytologist*,
769 127(2), 243–259. <https://doi.org/10.1111/j.1469-8137.1994.tb04276.x>
770 Grigoriev, I. V., Nikitin, R., Haridas, S., Kuo, A., Ohm, R., Otiillar, R., Riley, R., Salamov, A.,
771 Zhao, X., Korzeniewski, F., Smirnova, T., Nordberg, H., Dubchak, I., & Shabalov, I.
772 (2014). MycoCosm portal: Gearing up for 1000 fungal genomes. *Nucleic Acids*
773 *Research*, 42(Database issue), D699-704. <https://doi.org/10.1093/nar/gkt1183>
774 Hawdon, J. M., Narasimhan, S., & Hotez, P. J. (1999). Ancylostoma secreted protein 2:
775 Cloning and characterization of a second member of a family of nematode secreted
776 proteins from *Ancylostoma caninum*. *Molecular and Biochemical Parasitology*, 99(2),
777

778 149–165. [https://doi.org/10.1016/s0166-6851\(99\)00011-0](https://doi.org/10.1016/s0166-6851(99)00011-0)

779 Huerta-Cepas, J., Serra, F., & Bork, P. (2016). ETE 3: Reconstruction, Analysis, and
780 Visualization of Phylogenomic Data. *Molecular Biology and Evolution*, 33(6), 1635–
781 1638. <https://doi.org/10.1093/molbev/msw046>

782 Hunter, S., Apweiler, R., Attwood, T. K., Bairoch, A., Bateman, A., Binns, D., Bork, P., Das,
783 U., Daugherty, L., Duquenne, L., Finn, R. D., Gough, J., Haft, D., Hulo, N., Kahn, D.,
784 Kelly, E., Laugraud, A., Letunic, I., Lonsdale, D., ... Yeats, C. (2009). InterPro: The
785 integrative protein signature database. *Nucleic Acids Research*, 37(Database issue),
786 D211–D215. <https://doi.org/10.1093/nar/gkn785>

787 Kasparovsky, T., Milat, M.-L., Humbert, C., Blein, J.-P., Havel, L., & Mikes, V. (2003).
788 Elicitation of tobacco cells with ergosterol activates a signal pathway including
789 mobilization of internal calcium. *Plant Physiology and Biochemistry*, 41(5), 495–501.
790 [https://doi.org/10.1016/S0981-9428\(03\)00058-5](https://doi.org/10.1016/S0981-9428(03)00058-5)

791 Katoh, K., & Standley, D. M. (2013). MAFFT Multiple Sequence Alignment Software Version
792 7: Improvements in Performance and Usability. *Molecular Biology and Evolution*,
793 30(4), 772–780. <https://doi.org/10.1093/molbev/mst010>

794 Kelleher, A., Darwiche, R., Rezende, W. C., Farias, L. P., Leite, L. C. C., Schneiter, R., &
795 Asojo, O. A. (2014). Schistosoma mansoni venom allergen-like protein 4 (SmVAL4) is
796 a novel lipid-binding SCP/TAPS protein that lacks the prototypical CAP motifs. *Acta
797 Crystallographica Section D: Biological Crystallography*, 70(Pt 8), 2186–2196.
798 <https://doi.org/10.1107/S1399004714013315>

799 Kerekes, J., Desjardin, D., & Desjardin, D. (2009). A monograph of the genera Crinipellis and
800 Moniliophthora from Southeast Asia including a molecular phylogeny of the nrITS
801 region. *Fungal Diversity*, 37, 101–152.

802 Khoza, T. G., Dubery, I. A., & Piater, L. A. (2019). Identification of Candidate Ergosterol-
803 Responsive Proteins Associated with the Plasma Membrane of *Arabidopsis thaliana*.
804 *International Journal of Molecular Sciences*, 20(6). <https://doi.org/10.3390/ijms20061302>

805 Kim, D., Paggi, J. M., Park, C., Bennett, C., & Salzberg, S. L. (2019). Graph-based genome
806 alignment and genotyping with HISAT2 and HISAT-genotype. *Nature Biotechnology*,
807 37(8), 907–915. <https://doi.org/10.1038/s41587-019-0201-4>

808 Klempner, R. L., Sherwood, J. S., Tugizimana, F., Dubery, I. A., & Piater, L. A. (2014).
809 Ergosterol, an orphan fungal microbe-associated molecular pattern (MAMP).
810 *Molecular Plant Pathology*, 15(7), 747–761. <https://doi.org/10.1111/mpp.12127>

811 Kropp, B. R., & Albee-Scott, S. (2012). Moniliophthora aurantiaca sp. Nov., a Polynesian
812 species occurring in littoral forests. *Mycotaxon*, 120(1), 493–503.
813 <https://doi.org/10.5248/120.493>

814 Kurtz, S., Phillippy, A., Delcher, A. L., Smoot, M., Shumway, M., Antonescu, C., & Salzberg,
815 S. L. (2004). Versatile and open software for comparing large genomes. *Genome
816 Biology*, 5(2), R12. <https://doi.org/10.1186/gb-2004-5-2-r12>

817 Lemoine, F., Domelevo Entfellner, J.-B., Wilkinson, E., Correia, D., Dávila Felipe, M., De
818 Oliveira, T., & Gascuel, O. (2018). Renewing Felsenstein's phylogenetic bootstrap in
819 the era of big data. *Nature*, 556(7702), 452–456. [https://doi.org/10.1038/s41586-018-0043-0](https://doi.org/10.1038/s41586-018-
820 0043-0)

821 Liao, Y., Smyth, G. K., & Shi, W. (2014). featureCounts: An efficient general purpose
822 program for assigning sequence reads to genomic features. *Bioinformatics*, 30(7),
823 923–930. <https://doi.org/10.1093/bioinformatics/btt656>

824 Lochman, J., & Mikes, V. (2006). Ergosterol treatment leads to the expression of a specific
825 set of defence-related genes in tobacco. *Plant Molecular Biology*, 62(1–2), 43–51.
826 <https://doi.org/10.1007/s11103-006-9002-5>

827 Love, M. I., Huber, W., & Anders, S. (2014). Moderated estimation of fold change and

828 dispersion for RNA-seq data with DESeq2. *Genome Biology*, 15(12).
829 <https://doi.org/10.1186/s13059-014-0550-8>

830 Lozano-Torres, J. L., Wilbers, R. H. P., Warmerdam, S., Finkers-Tomczak, A., Diaz-
831 Granados, A., van Schaik, C. C., Helder, J., Bakker, J., Goverse, A., Schots, A., &
832 Smant, G. (2014). Apoplastic venom allergen-like proteins of cyst nematodes
833 modulate the activation of basal plant innate immunity by cell surface receptors.
834 *PLoS Pathogens*, 10(12), e1004569. <https://doi.org/10.1371/journal.ppat.1004569>

835 Manel, S., Perrier, C., Pratlong, M., Abi-Rached, L., Paganini, J., Pontarotti, P., & Aurelle, D.
836 (2016). Genomic resources and their influence on the detection of the signal of
837 positive selection in genome scans. *Molecular Ecology*, 25(1), 170–184.
838 <https://doi.org/10.1111/mec.13468>

839 Meinhardt, L. W., Costa, G. G. L., Thomazella, D. P., Teixeira, P. J. P., Carazzolle, M. F.,
840 Schuster, S. C., Carlson, J. E., Guiltinan, M. J., Mieczkowski, P., Farmer, A., Ramaraj,
841 T., Crozier, J., Davis, R. E., Shao, J., Melnick, R. L., Pereira, G. A., & Bailey, B. A.
842 (2014). Genome and secretome analysis of the hemibiotrophic fungal pathogen,
843 *Moniliophthora roreri*, which causes frosty pod rot disease of cacao: Mechanisms of
844 the biotrophic and necrotrophic phases. *BMC Genomics*, 15(1), 164.
845 <https://doi.org/10.1186/1471-2164-15-164>

846 Mohd As'wad, A. W., Sariah, M., Paterson, R. R. M., Zainal Abidin, M. A., & Lima, N. (2011).
847 Ergosterol analyses of oil palm seedlings and plants infected with *Ganoderma*. *Crop
848 Protection*, 30(11), 1438–1442. <https://doi.org/10.1016/j.cropro.2011.07.004>

849 Nguyen, L.-T., Schmidt, H. A., von Haeseler, A., & Minh, B. Q. (2015). IQ-TREE: A fast and
850 effective stochastic algorithm for estimating maximum-likelihood phylogenies.
851 *Molecular Biology and Evolution*, 32(1), 268–274.
852 <https://doi.org/10.1093/molbev/msu300>

853 Niveiro, N., Ramírez, N. A., Michlig, A., Lodge, D. J., & Aime, M. C. (2020). Studies of
854 Neotropical tree pathogens in *Moniliophthora*: A new species, *M. mayarum*, and
855 new combinations for *Crinipellis ticoi* and *C. brasiliensis*. *MycoKeys*, 66, 39–54.
856 <https://doi.org/10.3897/mycokeys.66.48711>

857 Nürnberg, T., Brunner, F., Kemmerling, B., & Piater, L. (2004). Innate immunity in plants
858 and animals: Striking similarities and obvious differences. *Immunological Reviews*,
859 198, 249–266. <https://doi.org/10.1111/j.0105-2896.2004.0119.x>

860 Oleksyk, T. K., Smith, M. W., & O'Brien, S. J. (2010). Genome-wide scans for footprints of
861 natural selection. *Philosophical Transactions of the Royal Society B: Biological Sciences*,
862 365(1537), 185–205. <https://doi.org/10.1098/rstb.2009.0219>

863 Patro, R., Duggal, G., Love, M. I., Irizarry, R. A., & Kingsford, C. (2017). Salmon provides fast
864 and bias-aware quantification of transcript expression. *Nature Methods*, 14(4), 417–
865 419. <https://doi.org/10.1038/nmeth.4197>

866 Prados-Rosales, R. C., Roldán-Rodríguez, R., Serena, C., López-Berges, M. S., Guarro, J.,
867 Martínez-del-Pozo, Á., & Di Pietro, A. (2012). A PR-1-like Protein of *Fusarium
868 oxysporum* Functions in Virulence on Mammalian Hosts. *The Journal of Biological
869 Chemistry*, 287(26), 21970–21979. <https://doi.org/10.1074/jbc.M112.364034>

870 Purdy, L., & Schmidt, R. (1996). STATUS OF CACAO WITCHES' BROOM: Biology,
871 Epidemiology, and Management. *Annual Review of Phytopathology*, 34(1), 573–594.
872 <https://doi.org/10.1146/annurev.phyto.34.1.573>

873 Ranwez, V., Douzery, E. J. P., Cambon, C., Chantret, N., & Delsuc, F. (2018). MACSE v2:
874 Toolkit for the Alignment of Coding Sequences Accounting for Frameshifts and Stop
875 Codons. *Molecular Biology and Evolution*, 35(10), 2582–2584.
876 <https://doi.org/10.1093/molbev/msy159>

877 Sambrook, J., & Russell, D. W. (2006). Purification of nucleic acids by extraction with

878 phenol:chloroform. *CSH Protocols*, 2006(1). <https://doi.org/10.1101/pdb.prot4455>

879 Schneiter, R., & Di Pietro, A. (2013). The CAP protein superfamily: Function in sterol export
880 and fungal virulence. *Biomolecular Concepts*, 4(5), 519–525.
881 <https://doi.org/10.1515/bmc-2013-0021>

882 Takahashi, H. (2002). Four new species of Crinipellis and Marasmius in eastern Honshu,
883 Japan. *Mycoscience*, 43(4), 343–350. <https://doi.org/10.1007/S102670200050>

884 Teixeira, Paulo J. P. L., Thomazella, D. P. T., Vidal, R. O., do Prado, P. F. V., Reis, O., Baroni,
885 R. M., Franco, S. F., Mieczkowski, P., Pereira, G. A. G., & Mondego, J. M. C. (2012).
886 The fungal pathogen Moniliophthora perniciosa has genes similar to plant PR-1 that
887 are highly expressed during its interaction with cacao. *PLoS One*, 7(9), e45929.
888 <https://doi.org/10.1371/journal.pone.0045929>

889 Teixeira, Paulo José Pereira Lima, Costa, G. G. L., Fiorin, G. L., Pereira, G. A. G., &
890 Mondego, J. M. C. (2013). Novel receptor-like kinases in cacao contain PR-1
891 extracellular domains. *Molecular Plant Pathology*, 14(6), 602–609.
892 <https://doi.org/10.1111/mpp.12028>

893 Teixeira, Paulo José Pereira Lima, Thomazella, D. P. de T., & Pereira, G. A. G. (2015). Time
894 for Chocolate: Current Understanding and New Perspectives on Cacao Witches'
895 Broom Disease Research. *PLoS Pathogens*, 11(10).
896 <https://doi.org/10.1371/journal.ppat.1005130>

897 Teixeira, Paulo José Pereira Lima, Thomazella, D. P. de T., Reis, O., Prado, P. F. V. do, Rio,
898 M. C. S. do, Fiorin, G. L., José, J., Costa, G. G. L., Negri, V. A., Mondego, J. M. C.,
899 Mieczkowski, P., & Pereira, G. A. G. (2014). High-Resolution Transcript Profiling of
900 the Atypical Biotrophic Interaction between Theobroma cacao and the Fungal
901 Pathogen Moniliophthora perniciosa. *The Plant Cell*, 26(11), 4245–4269.
902 <https://doi.org/10.1105/tpc.114.130807>

903 van Loon, L. C., Rep, M., & Pieterse, C. M. J. (2006). Significance of inducible defense-
904 related proteins in infected plants. *Annual Review of Phytopathology*, 44, 135–162.
905 <https://doi.org/10.1146/annurev.phyto.44.070505.143425>

906 Yang, Z. (2007). PAML 4: Phylogenetic analysis by maximum likelihood. *Molecular Biology
907 and Evolution*, 24(8), 1586–1591. <https://doi.org/10.1093/molbev/msm088>

908 Zhan, B., Liu, Y., Badamchian, M., Williamson, A., Feng, J., Loukas, A., Hawdon, J. M., &
909 Hotez, P. J. (2003). Molecular characterisation of the Ancylostoma-secreted protein
910 family from the adult stage of Ancylostoma caninum. *International Journal for
911 Parasitology*, 33(9), 897–907. [https://doi.org/10.1016/s0020-7519\(03\)00111-5](https://doi.org/10.1016/s0020-7519(03)00111-5)

912 Zhang, J., Nielsen, R., & Yang, Z. (2005). Evaluation of an Improved Branch-Site Likelihood
913 Method for Detecting Positive Selection at the Molecular Level. *Molecular Biology and
914 Evolution*, 22(12), 2472–2479. <https://doi.org/10.1093/molbev/msi237>

915 Zhao, X. R., Lin, Q., & Brookes, P. C. (2005). Does soil ergosterol concentration provide a
916 reliable estimate of soil fungal biomass? *Soil Biology and Biochemistry*, 37(2), 311–317.
917 <https://doi.org/10.1016/j.soilbio.2004.07.041>